INTERNATIONAL JOURNAL OF ADVANCE RESEARCH, IDEAS AND INNOVATIONS IN TECHNOLOGY

ISSN: 2454-132X
Impact factor: 4.295
(Volume 4, Issue 6)
Available online at: www.ijariit.com

Effect of waviness in the bearing on the life of rotating element

Pratibha Kale
pratibhakale13@yahoo.com
Yadavrao Tasgaonkar College of Engineering and Management, Karjat, Maharashtra

Santosh R. Wankhade
santosh.wankhede@tasgaokartech.com
Yadavrao Tasgaonkar College of Engineering and Management, Karjat, Maharashtra

ABSTRACT

Rotating structures or more general structures with constant but otherwise arbitrary velocity are important elements of machinery as rotor shafts and blades of the propellers, helicopters or the wind turbines. Vibrations in such structures require special attention. The vibrations may cause reduction in the life cycle of the rotating elements. But it must be noted that some vibration frequencies can be acceptable for the rotating element to sustain its life cycle. Sometimes, the vibrations may not have any impact on the life of the rotating element. That is the reason this study is undertaken. This project intends to study the impact of vibrations on the life cycle of the rotating elements, when the vibrations are due to waviness in the bearing. One of the main objectives of the project is to study the frequency at which the elements can be rotated with waviness in the bearing without affecting the life cycle of the elements. In this project, the 3D model of the bearing and rotating elements is modeled in modeling software and analyzed in ANSYS. Then the vibration frequencies for which the rotating element will sustain its life is analyzed using Vibration and Fatigue analysis in ANSYS. Then for that frequency, experimental analysis is conducted for evaluating the rpm of the rotating elements.

Keywords— *Vibration, Fatigue, Analysis, FEA*

1. INTRODUCTION

1.1 Fatigue failures

Fatigue is caused by cyclical stresses, and the forces that cause fatigue failures are substantially less than those that would cause plastic deformation. Confusing the situation even further is the fact that corrosion will reduce the fatigue strength of a material. The amount of reduction is dependent on both the severity of the corrosion and the number of stress cycles.

In diagnosing which mechanism caused the failure, a critical point to remember is that overload failures are generally caused by a single load application, while fatigue failures are always the result of a load applied repeatedly over many cycles. This means if the shaft failed as a result of an overload, the force that caused the failure was applied the instant before the shaft broke. Conversely, if fatigue was the culprit, the initial force may have been applied millions of cycles before the final failure occurred.

1.2 Vibration

In simplest terms, vibration in motorized equipment is merely the back and forth movement or oscillation of machines and components, such as drive motors, driven devices like pumps, compressors and the bearings, shafts, gears, belts and other elements that make up mechanical systems. Vibration in industrial equipment can be both a sign and a source of trouble. Other times, vibration just goes with the territory as a normal part of machine operation, and should not cause undue concern. Vibration is not always a problem. In some tasks, vibration is essential. Machines such as oscillating sanders and vibratory tumblers use vibration to remove materials and finish surfaces. Vibratory feeders use vibration to move materials. In construction, vibrators are used to help concrete settle into forms and compact fill materials. Vibratory rollers help compress asphalt used in highway paving. In other cases vibration is inherent in machine design. For instance, some vibration is almost unavoidable in the operation of reciprocating pumps and compressors, internal combustion engines and gear drives. In a well-engineered, well maintained machine, such vibration should be no cause for concern.

1.2.1 Effects of vibration

The effects of vibration can be severe. Unchecked machine vibration can accelerate rates of wear i.e. reduce bearing life and damage equipment. Vibrating machinery can create noise, cause safety problems and lead to degradation in plant working conditions. Vibration can cause machinery to consume excessive power and may damage product quality. In the worst cases, vibration can damage equipment so severely as to knock it out of service and halt plant production. Yet there is a positive aspect to machine vibration. Measured and analyzed correctly, vibration can be used in a preventive maintenance program as an indicator of machine condition, and help guide the plant maintenance professional to take remedial action before disaster strikes.

Following are the different vibration failure occurs in machine shafts:

1) **Transverse Vibrations**: Transverse vibrations are typically the result of an unbalanced drive shaft. A transverse vibration will occur once per every revolution of the drive shaft. This could be because of damage to the shaft, missing balance weights or foreign material stuck to the drive shaft.

2) **Torsional vibrations:** Torsional vibrations occur twice per revolution of the drive shaft. They could be due to excessive u-joint angles or a shaft not in phase with its design specifications. A yoke outside of its design phasing by just one spline can cause torsional vibration issues.
3) **Critical speed vibrations:** Critical speed vibrations occur when a drive shaft operates at an RPM too high in relation to its length, diameter and mass.
4) **Component failure:** Component failure of the drive shaft or the motor and transmission mounts can cause vibration. A failing u-joint is a prime example.

2. LITERATURE SURVEY

Ravindra A. Tarle, Nilesh K. Kharate, Shyam P. Mogal presented a paper on “Vibration Analysis of Ball Bearing” This paper addresses Design, Experimentation and Validation analysis of fault diagnosis of ball bearing related to rotor system. Detail analysis using FFT Methodology is done to find out the possible faults and finally validate with MATLAB software. Numbers of faults are identified and this will be validated for each fault. Faults are identified on single rotor system test rig. Experimental Evaluation & validation of faults are done to confirm results and finally effective solution is implemented to completely indicate faults of bearing which are being reported during validation process. In addition to this work has been done lubrication analysis by using FFT analyzer for bearing with lack of lubrication and bearing with lubrication. [1]

Sanjay Taneja presented a paper on “The Effect of Unbalance on Bearing Life”. In this paper the load and life calculation for the bearing are developed with considering the magnitude of eccentric unbalances. The influences of unbalances on the loads and life of the bearing are studied. The calculation and analysis results show that the radial loads on rolling element of the bearing fluctuate significantly under the actions of the unbalances of different parts of machines and the bearing life reduces regularly with the eccentric unbalances changing. This article focused not on machines that are supposed to vibrate as part of normal operation, but on those that should not vibrate like electric motors, rotary pumps and compressors, and fans and blowers. In these devices, smoother operation is generally better, and a machine running with zero vibration is the ideal. The result of overall study shows that small eccentric unbalances have small effect on the life of the water pump bearing, but if the eccentric unbalances, especially the fan unbalance, go beyond some threshold value, the life of the pump bearing would reduce sharply. In this paper the influences of the unbalance variations on the bearing life were studied. It was found that the unbalances will cause reduction of the bearing life and this effect would be remarkable if the unbalances increased to a certain level. The main component of the vibration is unbalance of the rotor and the rotor weight is nominal. [2]

E. M. Attia, A. N. Mohamed presented a paper on “Experimental Study on Vibrations of Shafts Suspended by Regular and Irregular Bore Journal Bearing”. This paper introduces an experimental model of whirling flexible shaft carrying a load at a mid-point and is supported by two identical journal bearings at its ends. Two types of journal bearings are fabricated, the first one its bore was made from regular surface and the second its bore was made from irregular surface. The analysis here is based on measuring the vibrations in the presence of regular and irregular bore journal bearing. Hammering and run - up test was made and analyzed for the two cases. Also effect of changing speed and load acting on each bearing was studied experimentally. An overall vibration is measured for different loads and the results were compared as the shaft is mounted by regular bore bearing or irregular type. The experimental results demonstrated the importance of using irregular surface for bore of journal bearings. From vibration analysis were concluded that, Vibrations level acting on shaft support depends on the load acting on the journal bearing irrespective of the shape of its bore. As the load increases the amplitude of vibrations increases especially for high speed of rotating shaft while at low speed, changing the load has no effect. The irregular bore of journal bearing minimizes the overall vibrations acting on rotating shafts for different speeds. Resonance frequencies are dependent on bore shape of journal bearing, since irregular shape minimizes the resonance frequencies. So it is better to use regular bore bearings for very high rotating speed of the shaft. The irregular bore of journal bearing minimizes the vibrations level during run-up of rotating shafts. The difference between vibrations level for the case of using regular and irregular bore bearing increases as the load and speed of shaft increases but the effect of load diminishes at low speed. [3]

Jaswinder Singh presented a paper on “Investigation of shaft rotor system using vibration monitoring technique for fault detection, diagnosis and analysis”. This paper involves design and fabrication of a rotor rig and investigations of vibrations at the bearings of the rig due to the effect of simulated faults. The line diagram of rotor test rig is also included in this paper. A solution has been presented to the unexpected downtime of a rotor shaft system. Experimentation has been carried on the model test rig to record the response of vibration amplitude at the two bearings by using transducers. The results presented show that the vibration amplitude varies in a sinusoidal or wavy form. Vibration amplitude depends solely on the distance of the bearing from the motor end of the shaft. The result shows that the test rig should not be operated beyond 4.8 mm vibration displacement amplitude. A critical speed of 4915 rpm for the test rig should also be avoided in order to prevent breakdown. Furthermore, the method used for analysis enabled early detection of the various effects of vibration signature such as imbalance, misalignment, and crack that may lead to downtime. [4]

3. NEED OF PROJECT

A shaft is a rotating member used to transmit power and rotational motion in machinery and mechanical equipment in various applications. It is a component usually used to connect other components of a drive train that cannot be connected directly because of distance or the need to allow for relative movement between them. It is supported by bearings and elements such as gears, belt and pulleys or sheaves, flywheels, clutches and sprockets are mounted on the shaft and are used to transmit power from the driving device. While in working condition shafts introduces to vibration due to various causes like unbalance, misalignment, wear looseness and various other reasons i.e. external undesirable excitations. Due to these undesirable vibrations, Shafts subjected to torsion, traverse or axial loads, acting in single or in combination with vibration causes severe stresses like torsion and shear stress in shaft. As due to excess vibration in shaft, it will cause to vibrate shaft to near about its natural frequency causing resonance to get introduced and it will cause the damage of shaft and hence the mechanical system. Also due to vibration in shaft, shaft introduces small cracks on its surface with increasing numbers and which reduces fatigue strength and life of shaft. Unchecked machine vibration can accelerate rates of wear i.e. reduce bearing life and damage equipment. Vibrating shaft can create noise, cause safety problems and lead to degradation in plant working conditions. Vibration can cause machinery to consume excessive power and may damage product quality. In the worst cases, vibration can damage equipment so severely as to knock it out of service and halt plant production. Hence it is important to study the vibration in shaft from various aspects and to conclude the effect of it on shaft life.

4. OBJECTIVES OF PROJECT

The key objectives of current work are as given below:

- Study of the vibrations in shafts, contribution of vibration in failure of shaft as a major cause.
- Finite element analysis of stresses in shaft due to undesirable vibration using ANSYS.
- Experimental analysis of shaft vibration and its effect on shaft life.
- Comparison of theoretical, FEA and experimental results for estimated effect of vibration on shaft life using FFT.

5. MATHEMATICAL CALCULATIONS

Input Parameters considered for basic design of shaft are,

Rotation of shaft = 1400 – 1500 RPM.

Power = 0.25 HP (180 Watt).

We know that power is given by formula,

$$P = \frac{2 \times \pi \times N \times T}{60} \quad (1)$$

Hence,

$$T = \frac{60 \times P}{2 \times \pi \times N}$$

Where,

P = Power transmitted by shaft in Watt (Nm/S)

T = Torque induced in shaft (Nm)

N = Rotation of Shaft (RPM)

Putting Values of P and N in above equation,

$$T = 1.228\ Nm$$

Hence Maximum motor torque,

$$T_{max} = 1.228\ Nm$$

Considering pulley on shaft for transmitting power from primary drive and shaft is under 25% overload.

Speed reduction ratio of pulley is taken, 1:4.

Hence by considering reduction ratio and overload, design torque will become,

$$T_{design} = T_{motor} \times 4.25$$

$$\therefore T_{design} = 5.219\ Nm$$

Hence shaft should be designed for above design torque of 5.219 Nm.

Using ASME code for designing of shaft, ASME code is based on maximum shear stress theory. According to this code, the permissible shear stress τ_{max} for the shaft without keyway is taken as 30% of yield strength in tension or 18% of ultimate tensile strength of the material, whichever is min.

At the top dead centre position, the thrust in the connecting rod will be equal to the force acting on piston

$$\therefore \tau_{max} = 0.30\ S_{yt}$$

$$\text{or } \tau_{max} = 0.18\ S_{ut}$$

If keyways are present, above values are to be reduced by 25%.

As in our setup there is no keyway, we will use:

$$\therefore \tau_{max} = 0.30\ Sty \text{ or } \tau_{max} = 0.18\ S_{ut}$$

Material selected for shaft is 40C8 (Low carbon steel) from standards of material for transmitting shafts, Engineering materials.

Mechanical properties of material for selected material,

Ultimate Tensile Strength (S_{ut}) - 660 MPa Yield Tensile Strength (S_{yt}) – 560 MPa

Modulus of Elasticity (E)–210 GPa Hardness (BHN) – 197 BHN Density of Material – 7850 Kg/m^3

Hence,

$$\tau_{max} = 0.30\ S_{yt}$$

$$\therefore \tau_{max} = 168\ MPa$$

Or

$$\tau_{max} = 0.18\ S_{ut}$$

$$\therefore \tau_{max} = 118.8\ MPa$$

Taking minimum value of maximum shear stress for safe design purpose,

Design shear stress will be τ_{max} =118.8 *MPa* Considering factor of safety (FOS) of 2,

$$\tau_{design} = 118.8$$

FOS

$$\therefore \tau_{design} = 59.4\ MPa$$

Considering equivalent torsional moment,

$$T_e = \sqrt{(K_b \times M_b)^2 + (K_t \times M_t)^2}$$

Where,

M_b: Bending moment of shaft (MPa).

K_b: Combined shack and fatigue factor for bending moment.

M_t: Torsional moment of shaft (MPa).

K_t: Combined shack and fatigue factor for torsional moment.

Considering Maximum torque induced in shaft and neglecting bending factor as transmission shaft are subjected to torque max time during its life.

$$T_e = \sqrt{(K_t \times M_t)^2}$$

Taking value of K_t = 1 to 3 for suddenly applied load from table for worse condition.

And M_t (MPa) as T_{design}(Nm) calculated before.

$$\therefore T_e = 15.657\ Nm$$

Based on Maximum shear stress theory,

$$T_{max} = \frac{\pi T_e d^3}{16}$$

$$\therefore d = 11.03\ mm$$

Taking standard shaft diameter from table of standards of steel industry for shafts,

$$d \cong 16\ mm$$

5.1 Equations of motion

The equations of motion for a Jeffcott rotor, with a cracked shaft, in a presence of gravity forces and unbalance excitation, and subjected to constant acceleration, can be expressed in inertial coordinate frame as follows:

$$\begin{pmatrix} M & 0 \\ 0 & M \end{pmatrix}\begin{Bmatrix} \ddot{z} \\ \ddot{y} \end{Bmatrix}+\begin{pmatrix} C & 0 \\ 0 & C \end{pmatrix}\begin{Bmatrix} \dot{z} \\ \dot{y} \end{Bmatrix}+\begin{pmatrix} K_{11} & K_{12} \\ K_{21} & K_{22} \end{pmatrix}\begin{Bmatrix} z \\ y \end{Bmatrix}=\begin{Bmatrix} Mg \\ 0 \end{Bmatrix}+M\varepsilon\begin{Bmatrix} \dot{\theta}^2\cos\theta+\ddot{\theta}\sin\theta \\ \dot{\theta}^2\sin\theta-\ddot{\theta}\cos\theta \end{Bmatrix} \quad (4)$$

where z and y are the displacements of the disk. The stiffness matrix $\mathbf{K}(\mathbf{q},t)$ (where $\mathbf{q}=(z\ \ y)^T$) is nonlinear, depending not only on time, but also on the position of the shaft center along the orbit.

The above equations of motion in the rotating coordinate can be written as

$$\begin{aligned}&\begin{pmatrix} M & 0 \\ 0 & M \end{pmatrix}\begin{Bmatrix} \ddot{\xi} \\ \ddot{\eta} \end{Bmatrix}+\begin{pmatrix} C & -2M\omega \\ 2M\omega & C \end{pmatrix}\begin{Bmatrix} \dot{\xi} \\ \dot{\eta} \end{Bmatrix}+\begin{pmatrix} K-f(\psi)\Delta K_\xi-M\omega^2 & -\omega C-M\alpha \\ \omega C+M\alpha & K-f(\psi)\Delta K_\eta-M\omega^2 \end{pmatrix}\begin{Bmatrix} \xi \\ \eta \end{Bmatrix}\\ &=Mg\begin{Bmatrix} \cos\Phi \\ -\sin\Phi \end{Bmatrix}+M\varepsilon\omega^2\begin{Bmatrix} \cos\beta \\ \sin\beta \end{Bmatrix}+M\varepsilon\alpha\begin{Bmatrix} \sin\beta \\ -\cos\beta \end{Bmatrix};\end{aligned} \quad (5)$$

where the transformation between the inertial and rotating coordinate frames takes the form:

$$\begin{pmatrix} z \\ y \end{pmatrix}=\begin{pmatrix} \cos\Phi & -\sin\Phi \\ \sin\Phi & \cos\Phi \end{pmatrix}\begin{pmatrix} \xi \\ \eta \end{pmatrix} \quad (6)$$

Incorporating the hinge model for small cracks into Eq. (5) ($\Delta K_\eta=0$), normalizing displacements with respect to static deflection, and using nondimensional time yields:

$$\begin{aligned}&\begin{bmatrix} 1 & 0 \\ 0 & 1 \end{bmatrix}\begin{Bmatrix} \bar{\xi}'' \\ \bar{\eta}'' \end{Bmatrix}+\begin{bmatrix} 2\zeta & -2\frac{\omega}{\omega_n} \\ 2\frac{\omega}{\omega_n} & 2\zeta \end{bmatrix}\begin{Bmatrix} \bar{\xi}' \\ \bar{\eta}' \end{Bmatrix}+\begin{bmatrix} 1-f(\psi)\Delta K-\frac{\omega^2}{\omega_n^2} & -2\zeta\frac{\omega}{\omega_n}-\frac{\alpha}{\omega_n^2} \\ 2\zeta\frac{\omega}{\omega_n}+\frac{\alpha}{\omega_n^2} & 1-\frac{\omega^2}{\omega_n^2} \end{bmatrix}\begin{Bmatrix} \bar{\xi} \\ \bar{\eta} \end{Bmatrix}=\\ &\begin{Bmatrix} \cos\Phi \\ -\sin\Phi \end{Bmatrix}+\begin{Bmatrix} \frac{\varepsilon}{\eta_{st}}\frac{\omega^2}{\omega_n^2}\cos\beta+\frac{\varepsilon}{\eta_{st}}\frac{\alpha}{\omega_n^2}\sin\beta \\ \frac{\varepsilon}{\eta_{st}}\frac{\omega^2}{\omega_n^2}\sin\beta-\frac{\varepsilon}{\eta_{st}}\frac{\alpha}{\omega_n^2}\cos\beta \end{Bmatrix};\end{aligned} \quad (7a)$$

where here $f(\psi)$ is a rectangular steering function (see Fig. 2(a)).

Similarly, one can incorporate into the equations of motion (Eq. (5)) the model for deep crack, assuming $\Delta K_\eta=\frac{\Delta K_\xi}{6}$, and Meyes[6] modified steering function $f(\psi)=\frac{1+\cos(\psi)}{2}$ (see Fig. 2(a)), and write that

$$\begin{aligned}&\begin{bmatrix} 1 & 0 \\ 0 & 1 \end{bmatrix}\begin{Bmatrix} \bar{\xi}'' \\ \bar{\eta}'' \end{Bmatrix}+\begin{bmatrix} 2\zeta & -2\frac{\omega}{\omega_n} \\ 2\frac{\omega}{\omega_n} & 2\zeta \end{bmatrix}\begin{Bmatrix} \bar{\xi}' \\ \bar{\eta}' \end{Bmatrix}+\begin{bmatrix} 1-f(\psi)\Delta K-\frac{\omega^2}{\omega_n^2} & -2\zeta\frac{\omega}{\omega_n}-\frac{\alpha}{\omega_n^2} \\ 2\zeta\frac{\omega}{\omega_n}+\frac{\alpha}{\omega_n^2} & 1-\frac{f(\psi)\Delta K}{6}-\frac{\omega^2}{\omega_n^2} \end{bmatrix}\begin{Bmatrix} \bar{\xi} \\ \bar{\eta} \end{Bmatrix}=\\ &\begin{Bmatrix} \cos\Phi \\ -\sin\Phi \end{Bmatrix}+\begin{Bmatrix} \frac{\varepsilon}{\eta_{st}}\frac{\omega^2}{\omega_n^2}\cos\beta+\frac{\varepsilon}{\eta_{st}}\frac{\alpha}{\omega_n^2}\sin\beta \\ \frac{\varepsilon}{\eta_{st}}\frac{\omega^2}{\omega_n^2}\sin\beta-\frac{\varepsilon}{\eta_{st}}\frac{\alpha}{\omega_n^2}\cos\beta \end{Bmatrix}\end{aligned} \quad (7b)$$

In the above equations the following definitions and nondimensional variables were employed (see Nomenclature section):

$$\omega_n^2=\frac{K}{M},\quad \Delta K=\frac{\Delta K_\xi}{K},\quad \zeta=\frac{C}{2M\omega_n},\quad \gamma=\frac{\alpha}{\omega_n^2}$$

$$\eta_{st}=\frac{Mg}{K}=\frac{g}{\omega_n^2},\quad \bar{\xi}=\frac{\xi}{\eta_{st}},\quad \bar{\eta}=\frac{\eta}{\eta_{st}},\quad \tau=\omega_n t,\quad \frac{\omega}{\omega_n}=\gamma\tau$$

$$\omega=\omega_0+\alpha t=\alpha t,\ \text{for } \omega_0=0$$

$$\Phi=\Phi_0+\omega_0 t+\frac{\alpha t^2}{2}=\frac{\gamma\tau^2}{2},\ \text{for } \Phi_0=0$$

$$\xi=\frac{g\bar{\xi}}{\omega_n^2},\quad \eta=\frac{g\bar{\eta}}{\omega_n^2},\quad \dot{\xi}=\frac{g\bar{\xi}'}{\omega_n},\quad \dot{\eta}=\frac{g\bar{\eta}'}{\omega_n}$$

$$\ddot{\xi}=g\bar{\xi}'',\quad \ddot{\eta}=g\bar{\eta}''$$

6. MODELLING AND ANALYSIS

Fusion 360 software is used for modelling the set up for the shaft, bearing. Model is shown in the image below in figure 1.

Fig. 1: Set up three dimensional model

Model then is imported in the ANSYS Workbench and solid model is created using Element type 185. Bearing, shafts, frame is created. Mass element of the equivalent mass at the cg of pulley as well as motor is created to represent it. Mass of the total set up is calculated to be 9.1 kg. Meshed model image is shown in the figure below in figure 2. Motor we have attached to the setup is specified to have maximum rpm of 7000 RPM which makes the maximum frequency of the loading for the component as follow.

Maximum frequency = RPM/60

So maximum loading frequency in the set up can be said to be 116.7 Hz. Further reduction in the loading frequency occurs while transmitting from smaller pulley to the larger one.

Fig. 2: Meshed model for set up

With fixing all the four columns of the set-up from below, natural frequencies for the set up are calculated using ANSYS software. Below are the results for the analysis performed in figure 3.

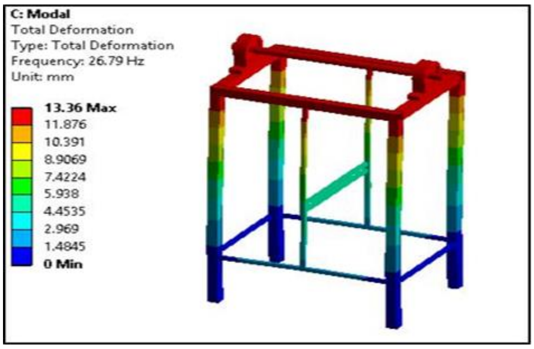

Fig. 3: First mode shape plot at 26.79 Hz

First mode shape of the modal analysis is shown in the figure no 3 and it shows natural frequency of 26.8 Hz in the horizontal direction buckling of the set-up.

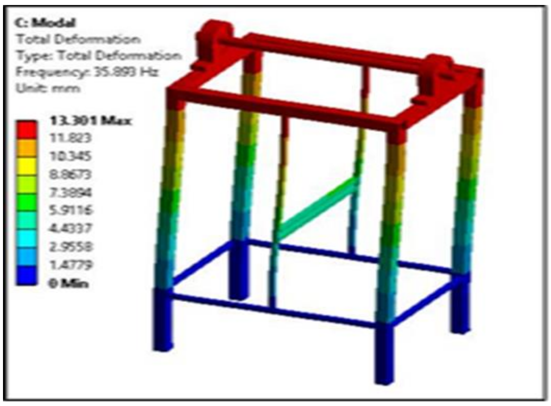

Fig. 4: Second mode shape plot at 35.9 Hz

Then next frequency plot of second mode shape is shown in the figure 4 which shows frequency of 35.9 Hz. Result table for frequencies is shown in the results and discussion to show first 6 natural frequencies of the system.

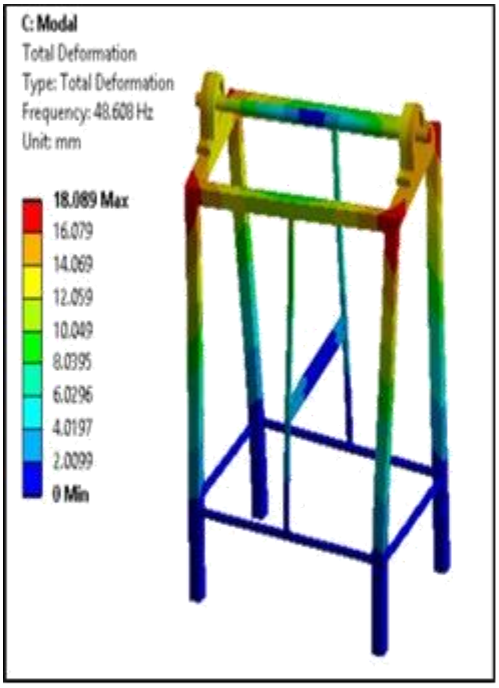

Fig. 5: Mode shape plot at mode 3 at 48.6 Hz

Mode shape 3 for the third natural frequency of the system is shown in the figure 5 which shows twisting mode of the vibration of bearing set up.

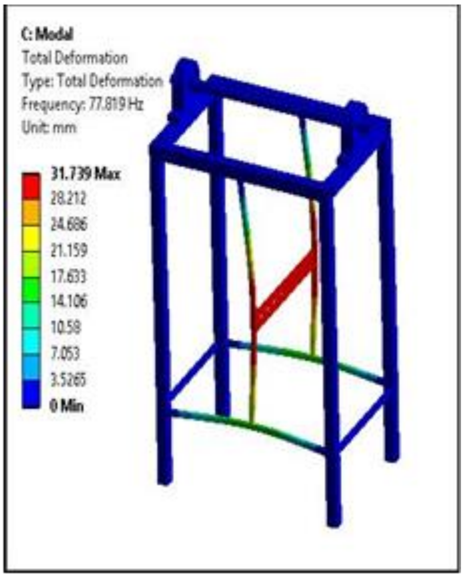

Fig. 6: Mode shape plot at mode 4 at 77.8 Hz

The next mode shape of 77.8 HZ frequency shown in the next image is the last frequency below the loading frequency of the motor. Major vibrations will be caused by the loading frequency of the motor.

Harmonic Analysis

Harmonic analysis is performed on the set up model with the loading measured at the motor mounting bars and torsional loading is applied to the shaft with harmonic sine sweep of frequencies ranging from 0 to 100 Hz with assumed damping of 2.5 %, so that loading covers all the natural frequencies of the system below loading frequency.

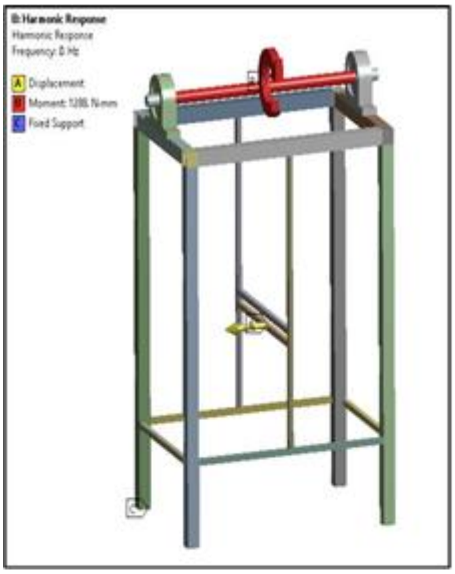

Fig. 7: Boundary conditions of harmonic analysis

Below are the figures from the analysis. Design torque of 1.288 N-m is applied to the shaft and motor mounting is applied with the deformation of 0.5 mm harmonically. 5 degrees of slip between the pulley and the belt is assumed and torque is considered 5 degrees out of phase than motor vibrations.

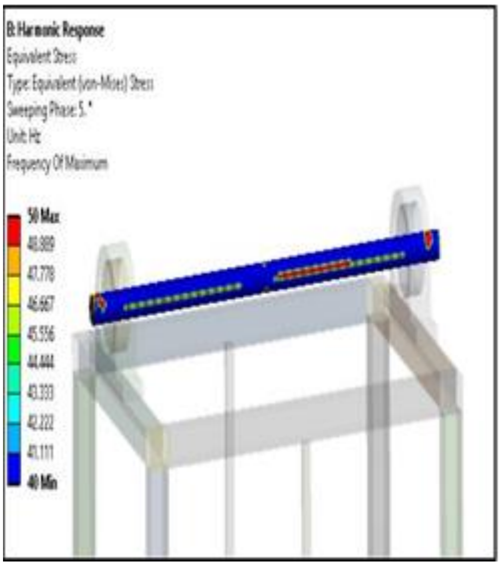

Fig. 8: Frequency of the maximum stress

Results for the analysis are shown in the figure.

Frequency of the maximum stress is plotted for the shaft and it shows that most of the shaft has its maximum stress observed at the frequency of 40 Hz and 50 Hz.

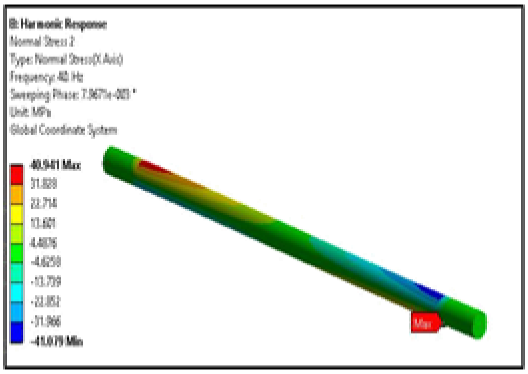

Fig. 9: Maximum von mises stress over frequencies in Harmonic analysis

Stress plot for the maximum stress over all the frequencies is plotted below. Von mises stress plot shows maximum stress of 40.94 MPa

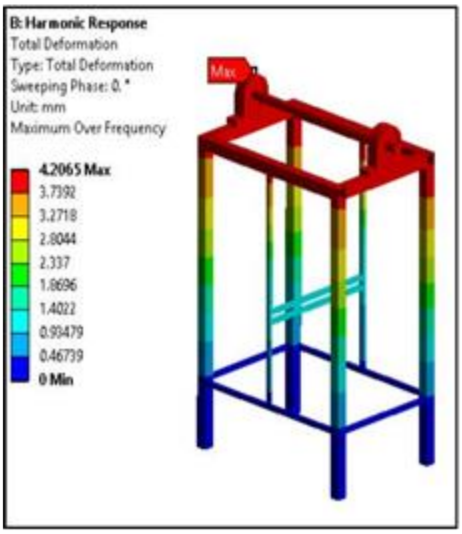

Fig. 10: Total deformation plot maximum over frequency

Total deformation plot shows the maximum deformation of 4.2 mm.

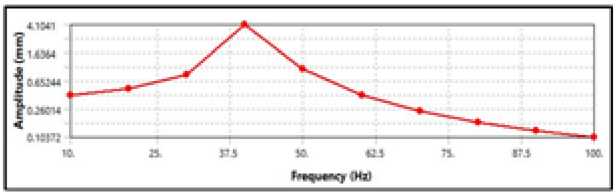

Fig. 11: Deformation vs. frequency graph

SN curve table shown for the steel are shown below in table 1. Stress response at the 40 Hz frequency shows the alternating stress of 82 MPa in shaft mounted in bearing with ideal conditions. So shaft will have infinite life in vibrations. As per SN curve table for the steel below 82 MPa alternating stress.

Table 1: Alternating stress vs Number of cycles

Alternating Stress MPa	Cycles	Mean Stress MPa
3999	10	0
2827	20	0
1896	50	0
1413	100	0
1069	200	0
441	2000	0
262	10000	0
214	20000	0
138	1.00E+05	0
114	2.00E+05	0
86.2	1.00E+06	0

Frequency responses in the ideal condition of the bearing are also noted as shown in the figures below.

Fig. 12: Frequency responses location for 4 and 5

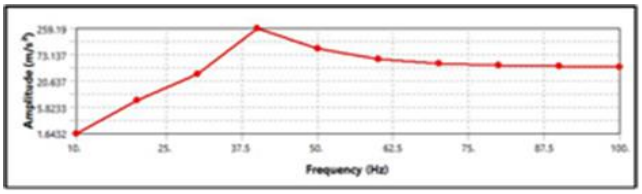

Fig. 13: Frequency response 4

It shows maximum frequency response at 40 Hz which is observed as 259.19 m/s^2. There is hardly any difference in the both responses of the bearing due to symmetry of the boundary conditions. So both responses are similar.

After ideal analysis of FEA for model is done, actual vibrations at the field on the bearing are measured and performance is compared with the ideal analysis.

Response Analysis

After harmonic analysis with the given loading conditions the vibrations on the bearing in actual running condition are measured and are used as an input for the response analysis. Stress in the shaft due to response analysis is found out and its position in the SN curve is checked. Different measured conditions are applied to the response analysis. Starting with the first no damage bearing condition.

Boundary conditions to the all response analysis is shown in the image below.

Fig. 14: Boundary conditions for the response analysis

At location A bearing vibrations are applied as an input as per measurements from the field on the set up. At location B where there was fixed support in harmonic analysis maximum displacement over the frequencies is applied. Stress results for the different cases are calculated using response analysis result post processing as shown below.

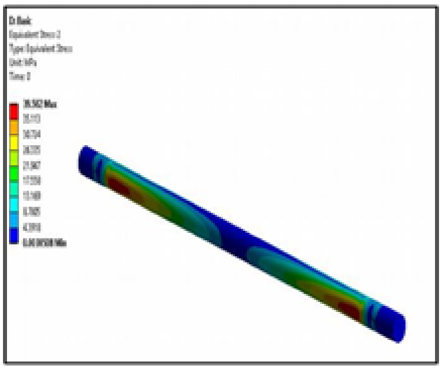

Fig. 15: Von mises stress plot response at bearing ball missing response.

Von mises stress observed increased from 39.5MPa to 43.1 MPa. SN curve still will show that there is just less than the infinite limit. At stress range of 86.2 MPa cycles will be close to 1E6.

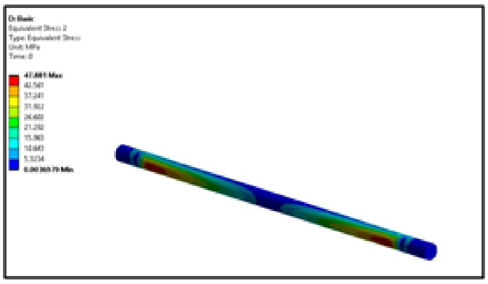

Fig. 16: von Mises stress plot at bearing contamination of grease

Maximum shear stress of 47.8 MPa is observed in the figure resulting stress range of 95.6 MPa of alternating stress. It will have finite fatigue life. Between 1E5 to 1E6.

This shows contamination affects the shaft life more than the missing ball defect.

7. EXPERIMENTAL VALIDATION PLAN

For experimental testing Single channel FFT analyzer is used. Probe of FFT analyzer is mounted on pedestal bearing.

Fig. 17: Experimental Setup

Fig. 18: Experimental Testing using FFT Analyzer

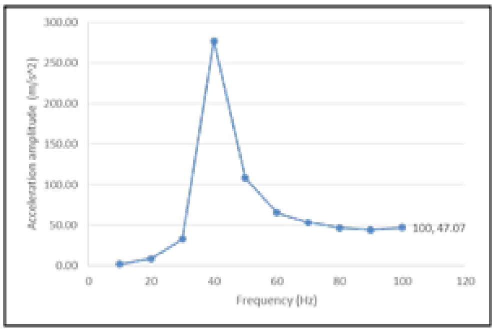

Fig. 19: Vibration reading for experimental set up no defect

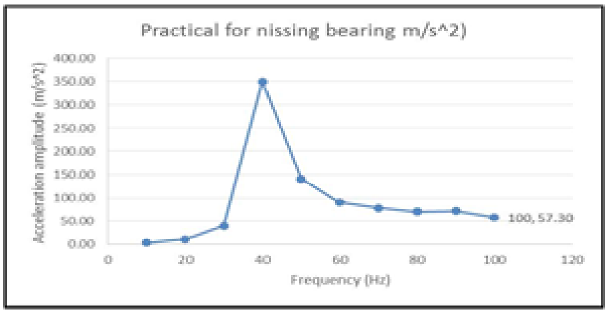

Fig. 20: Graph of acceleration amplitude vs Frequency bearing ball missing

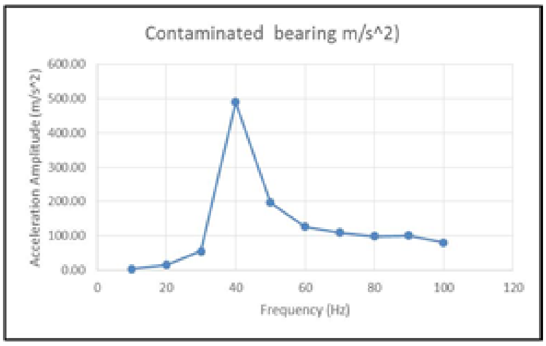

Fig. 21: Graph of acceleration amplitude vs Frequency bearing contaminated with oil

8. RESULTS AND DISCUSSION

Table 2 for the result summary of FEA and practical is given below.

Table 2: Summary of FEA and practical

Bearing Condition	Stress Range on Shaft in MPa
No damage bearing	79
One ball removed bearing	86.2
Bearing with oil contaminant	94

Results of the response analysis for no defect bearings and harmonic analysis done on the assembly are both within limit.

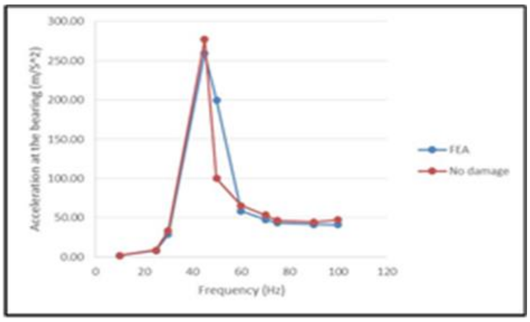

Fig. 22: Comparison between FEA analysis results and actual practice for first no damage condition

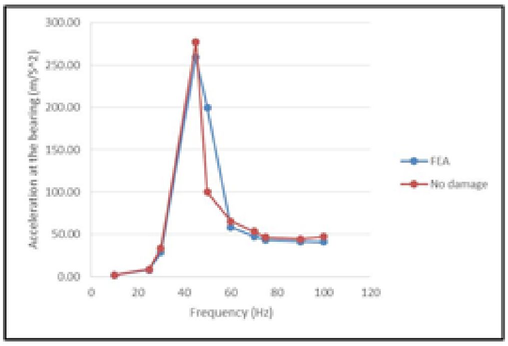

Fig. 23: Comparison of the practical testing for different bearing vibrations

Comparison of the all the bearing vibration plots shows us that contamination in the bearing grease causes higher vibration amplitudes at the similar frequencies.

Results are almost similar with testing and manufacturing.

9. CONCLUSION

Vibration in the bearing can cause the stresses in the shaft mounted on those bearing. Without any damage response analysis shows 39.502 MPa stresses. With ball missing the stresses increased by 3.591 MPa due to slight increase in the vibration of the bearing. Third bearing defect, the defect in the bearing contamination causes high stress up to 47.881 MPa bu stress is more than the endurance limit of shaft. Thus it can be concluded that the defect in the bearing by one ball removed e does not have any effect on the life of the shaft but in bearing contaminated with oil will have effect on life of shaft.

10. FUTURE SCOPE

- Different bearing mounting types can be studied and their effect on the vibration can be analyzed.
- Different materials for mounting of bearing for dampening of the vibrations can be studied.
- Fatigue analysis and testing can be performed on the complete set up.

11. REFERENCES

[1] Ravindra A. Tarle, Nilesh K. Kharate, Shyam P. Mogal, "Vibration Analysis of Ball Bearing", International Journal of Science and Research (IJSR), ISSN (Online): 2319 – 7064, Paper ID: SUB154835, Volume 4 Issue 5, May 2015.

[2] Sanjay Taneja, "The Effect of Unbalance on Bearing Life", IOSR Journal of Mechanical and Civil Engineering (IOSRJMCE), ISSN: 2278-1684 Volume 1, Issue 2 (July-Aug 2012), PP 47-54.

[3] E.M.Attia, A.N .Mohamed, "Experimental Study on Vibrations of Shafts Suspended by Regular and Irregular Bore Journal Bearing", Alexandria University- Faculty of Engineering -Department of mechanical engineering, E-ISSN: 2224-3429, Volume 11, 2016.

[4] Jaswinder Singh, "Investigation of shaft rotor system using vibration monitoring technique for fault detection, diagnosis and analysis", Mechanica Confab, Vol. 2, No. 2, February-March 2013 ISSN: 2320-2491.

[5] Jerzy T. Sawicki, Xi Wu, George Y. Baaklinit, Andrew L. Gyekenyes, "Vibration based crack diagnosis in rotating shafts during acceleration through resonance", NDE and Health Monitoring of Aerospace Materials and Composites II, SPIE Vol. 5046 (2003)

[6] Prof. D. R. Satpute, Prof. S. B. Belkar, Prof. M. S. Mhaske, "Multiple Cracks Effects on Vibration Characteristics of Shaft Beam", International Journal of Engineering Research and General Science Volume 3, Issue 1,January-February, 2015 ISSN 2091-2730.

[7] Sumit P. Raut, Laukik P. Raut, "A Review of Various Techniques Used for Shaft Failure Analysis", International Journal of Engineering Research and General Science Volume 2, Issue 2,Feb-Mar 2014 ISSN 2091-2730.

[8] Ali Vaziri, Prof. M. J. Patil, "Vibration analysis of a cracked shaft", International Journal of Advanced Engineering Technology, International Journal of Advanced Engineering Technology IJAET/Vol. IV/ Issue II/April-June, 2013/103-104 E-ISSN 0976-3945.

[9] Kundan Kumar, Prof. K. H. Munde, "Condition monitoring vibration Analysis of default shaft", International Journal of Science, Engineering and Technology Research (IJSETR) Volume 4, Issue 4, April 2015,ISSN: 2278 – 7798.

